


# Improved wideband phase balancing SIW unequal power divider design for the low side-lobe array antennas

Shahriar Hasan Shehab<sup>1</sup>  | Jiewei Feng<sup>1</sup> | Nemai Karmakar<sup>1</sup> | Emran Md Amin<sup>2</sup> | Jeffrey Walker<sup>3</sup>

<sup>1</sup>Department of Electrical and Computer Systems Engineering, Monash University, Melbourne, Australia

<sup>2</sup>Australian Communications and Media Authority, Melbourne, Australia

<sup>3</sup>Department of Civil Engineering, Monash University, Melbourne, Australia

## Correspondence

Shahriar Hasan Shehab, Department of Electrical and Computer Systems Engineering, Monash University, Melbourne, Australia.  
Email: [shahriar.shehab@monash.edu](mailto:shahriar.shehab@monash.edu)

## Funding information

Australian Research Council (ARC), Grant/Award Number: DP160104233

## Abstract

In this paper, an eight-way substrate integrated waveguide unequal power divider with an enhanced co-phase bandwidth is presented, and demonstrated a potential application for the Ku-band radiometer antennas. The proposed divider design is based on the  $-35$  dB Chebyshev beam-shaping algorithm to achieve at minimum  $-25$  dB of antenna side-lobe level (SLL) and high beam efficiency ( $>90\%$ ). Investigations on different unequal power splitting techniques are discussed, and an efficient method for the unequal power division is proposed, exhibiting improved co-phase bandwidth and wideband matching. The proposed unequal eight-way power divider demonstrates a wider co-phase bandwidth of 10% within  $10^\circ$  phase error and the  $-15$  dB return loss bandwidth of 36.8%. Furthermore, the proposed unequal divider is integrated with eight longitudinal slot radiators, designed at 18.7 GHz and exhibits low radiation loss (better than  $-1.3$  dB). The antenna measurement results exhibit a symmetrical fan beam radiation pattern and satisfied the goal of  $-25$  dB SLL, resulting high beam efficiency of 97% and gain of 13.45 dBi. Therefore, the proposed unequal power divider technique shows the potential to be utilised in the low SLL antenna array designs for an accurate brightness temperature measurement of radiometer systems. The application of this technique can be further extended to radar and satellite/wireless communications.

## 1 | INTRODUCTION

Low side-lobe level (SLL) array antennas are highly demanded in high-performance radar and communication systems (especially point to point), for the purposes of improving spatial/spectral efficiency, or decreasing susceptibility to inference/clutter [1–4]. Low SLL is also stringently required in radiometer antennas. In particular, passive radiometer systems are dominant in remote soil-moisture-sensing technology. Remote-sensing radiometers receive weak microwave and mm-wave noise-like signal from the Earth's thermal radiation. The received signal is filtered, amplified and processed to the equivalent thermal radiation (brightness temperature) which is a vital dataset for soil moisture retrieval algorithm. To capture accurate soil moisture information within the scanning footprint, the radiometer system needs an antenna array with high beam efficiency ( $>90\%$ ) [5]. The required antenna array comprises highly efficient radiating elements integrated with

balanced phase unequal power dividers to suppress the antenna SLL. The lower SLL improves the antenna beam efficiency, resulting in the detection of the thermal radiation being mostly contributed from its scanning footprint (main beam), and reducing the unwanted signals from antennas' side lobes and back lobe for better accuracy. Metallic waveguides are quite attractive due to their low loss and high-Q factors [6] in microwave frequency bands. However, they are bulky metallic structures and exhibit significant fabrication complexity at high microwave and mm-wave frequency bands. Besides, microstrip patch antennas have many inherent salient advantages for satellite communications such as light weight, low cost, high-Q radiators, and conformal to the body of revolution of the payloads [7]. Nevertheless, at a higher frequency, significant radiation leakage from the feed lines reduces the antenna efficiency. Substrate integrated waveguide (SIW) technology, proposed in [8], shaped the bulky metallic waveguides into planar form, by adding two rows of conducting vias in parallel

This is an open access article under the terms of the Creative Commons Attribution License, which permits use, distribution and reproduction in any medium, provided the original work is properly cited.

© 2020 The Authors. *IET Microwaves, Antennas & Propagation* published by John Wiley & Sons Ltd on behalf of The Institution of Engineering and Technology.

to form the shield of electric fields. The investigation on the SIW was initiated with the name of 'laminated waveguide' in [9], and then significant development has been reported on microwave and mm-wave circuit components such as antennas, power dividers/combiners, mixers, multiplexers etc.

The power divider is a fundamental block of an antenna array system, operating in either equal or unequal split ratios. Several SIW divider topologies which include series [10], corporate [11–13], multimode imaging [14], half-mode SIW (HMSIW) [15], magic-T [16], radial cavity [17], Wilkinson [18], and Gysel [19] have been reported. Each of the configurations has distinctive performance characteristics in terms of the return loss and co-phase bandwidth, phase and amplitude balance, insertion loss, and isolation. Antenna array feed networks with unequal split ratios require higher co-phase bandwidth to avoid beam squint over the operating frequency bandwidth. Series and corporate dividers are comparatively suitable for antenna array configurations. Despite the compactness, series dividers provide alternating phase and enormously poor co-phase bandwidth [10] which increases frequency sensitivity to the beam pattern. In contrast, corporate dividers provide higher return loss and co-phase bandwidth with the cost of compactness and moderate isolation, which can be further improved by using multilayer configuration and additional resistive branches between ports, respectively. An unequal power divider was presented in [12], which has particularly emphasised on improving the co-phase bandwidth. A co-phase bandwidth of 2% (considering 7° phase error) with the maximum power difference of ~17 dB (i.e., 100:20) was reported. However, this power divider design resulted in lower (−15 dB) return loss bandwidth of ~9%.

Therefore, the investigation on the improvement of the co-phase bandwidth along with the impact on the return loss bandwidth for the SIW unequal power divider design was highlighted in this work to improve the antenna beam stability for (and not limited to) the radiometer application. Section 2 demonstrates the investigation on non-uniform SIW power divider design, we propose a new design procedure targeting higher split ratios with minimum phase imbalance along with the required compensation technique. The proposed unequal power divider responses are validated with measurement results are reported in Section 3. In Section 4, an 8×1 SIW antenna array is designed with the proposed power divider and the measurements will be reported and discussed. Finally, Section 5 provides the conclusion of this work.

## 2 | SIW NON-UNIFORM POWER DIVIDER DESIGN

This section presents a systematic design procedure of an unequal SIW power divider design and a phase balancing technique. The design starts with an analysis of an unequal Y-junction power divider to achieve high split ratios with low phase imbalance. Henceforth, the phase balancing method is described to obtain a balanced phase response. Taconic-TLX 8 ( $\epsilon_r=2.55$  and  $\tan\delta = 0.0019$ ) with thickness of 0.5 mm was

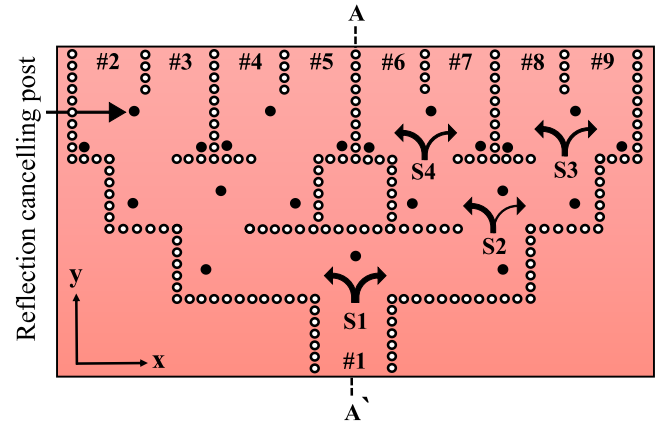


**FIGURE 1** Substrate integrated waveguide eight-way corporate power divider model

chosen as the substrate material for low dielectric loss. The designs were analysed with the commercial full-wave electromagnetic solver CST Microwave Studio.

### 2.1 | Unequal Y-divider design

Figure 1 shows an eight-way corporate SIW power divider model. The SIW width was calculated to be 7.5 mm, following the guidelines provided in [20]. The cut-off frequency was selected to be at 12 GHz to keep in the antenna operating frequency (18.7 GHz) within its dominant mode, which resulted in minimum multi-modal dispersion. The via diameter ( $d$ ) was chosen to be 0.5 mm and the spacing between two adjacent via's ( $s$ ) was 0.8 mm, to comply with the design rule of  $s/d < 2$ . The design of conventional equal T- and Y-dividers was performed by adding additional inductive vias at the port junctions. The y-position was primarily set to  $\lambda_g/4$  position, both the position and the diameter of the additional posts were slightly optimised to 3.4 and 0.5 mm, respectively, for better port matching. Later, for the unequal power division, the Chebyshev distribution algorithm [21] was used to calculate the port coefficients for the required SLL. For a uniformly spaced array with amplitude that is symmetrical about the centre, the array factor (AF) can be written as

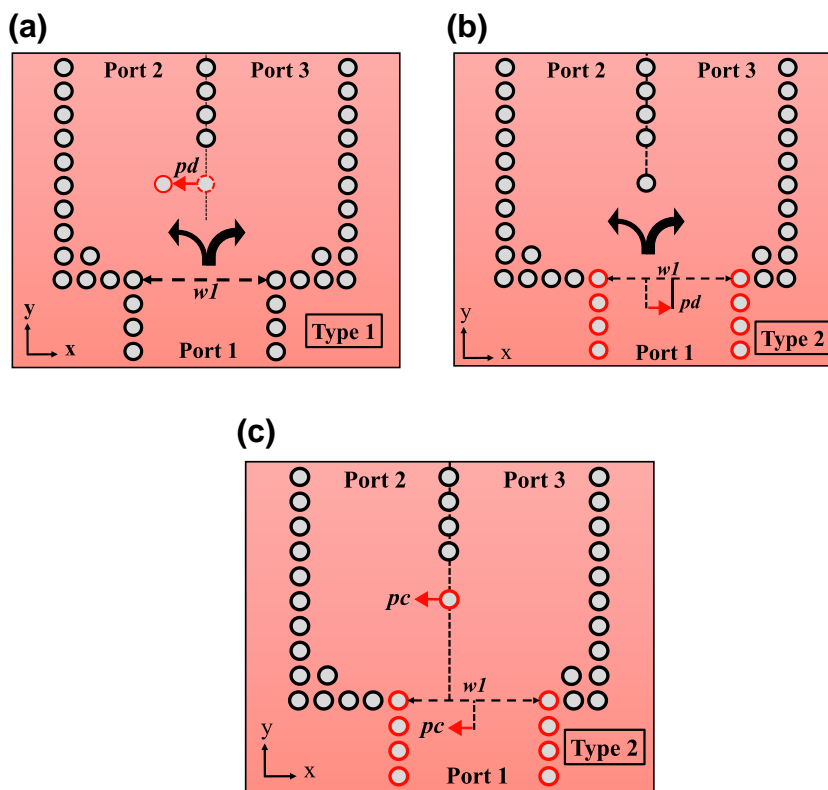
$$AF = \begin{cases} 2 \sum_{m=1}^{N/2} I_m \cos \left[ \left( m - \frac{1}{2} \right) u \right], & \text{for } N \text{ even} \\ \sum_{m=1}^{(N+1)/2} I_m \cos [(m-1)u], & \text{for } N \text{ odd} \end{cases} \quad (1)$$

For a linear array of eight radiating elements ( $N = 8$ ), the excitation coefficients ( $I_m$ ) were calculated and presented in Table 1 including the required voltage division ratios for each stage.

To apply the Chebyshev coefficients, the eight-way power splitter was divided into four stages (i.e., S1–S4) as shown in Figure 1. Table 1 shows that the maximum 100:37 ratio is

**TABLE 1** Chebyshev excitation coefficients and corresponding voltage division ratios per stage

SLL	Port coefficients							
	#2	#3	#4	#5	#6	#7	#8	#9
-35 dB	0.19	0.46	0.78	1	1	0.78	0.46	0.19
	Stage S3 (41:100)		Stage S4 (78:100)		Stage S4 (100:78)		Stage S3 (100:41)	
	Stage S2 (37:100)				Stage S2 (100:37)			
	Stage S1 (100:100)							

**FIGURE 2** Y-divider: (a,b) unequal power division methods and (c) phase balancing technique

required to achieve  $-35$  dB SLL. The first splitting stage (S1) requires an equal split ratio due to the symmetric distribution with respect to the centre line (A–A'), whereas the rest of the stages S2, S3 and S4 require unequal split ratios. Accordingly, the voltage division ratio of each stage is normalised based on the higher portion side. For example, for Stage S2, 37:100 is computed based on

$$\text{Ratio of S2} = \frac{I_2 + I_3}{I_4 + I_5} \times 100\% = \frac{0.19 + 0.46}{0.78 + 1} \times 100\% = 37\% \quad (2)$$

The conventional method of having unequal power split in Y- or T-dividers is to offset the inductive post position in the positive  $x$ -direction, which also causes phase imbalance between output ports. Then, conventional method to compensate such phase imbalance is to change the path length.

First, the conventional method (Type 1) was followed as shown in Figure 2(a), to offset the inductive post (as highlighted) in the  $-x$ -direction. It can be observed from Figure 3 that the maximum 100:40 split ratio can be obtained. The ratio bandwidth degraded to 36% due to the port mismatch with increasing split ratio. Additionally, the maximum phase imbalance was nearly  $58^\circ$ , which requires further compensation. Consequently, additional posts were required to nullify such significant phase imbalance, which will further affect the port matching and increase the design complexity. Instead, here we propose a new method (Type 2) as shown in Figure 2(b), the input port (as highlighted) was moved in the  $+x$ -direction ( $pd$ ), while keeping the inductive post stationary. It can be observed that a maximum 100:37 split ratio could be obtained with a phase imbalance of  $23^\circ$ . Additionally, the ratio bandwidth was hardly deviated, which remained above 50%. Comparing the responses between the two methods, the proposed method (Type 2) outperforms and is used as the first

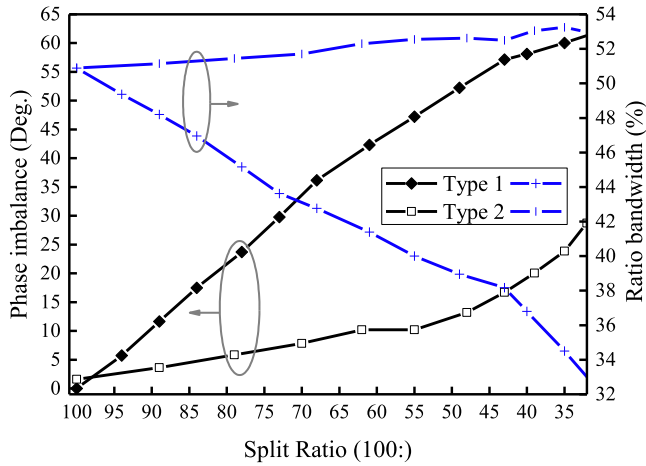


**FIGURE 3** Effects on phase balance and bandwidth for different split ratios on Y-divider

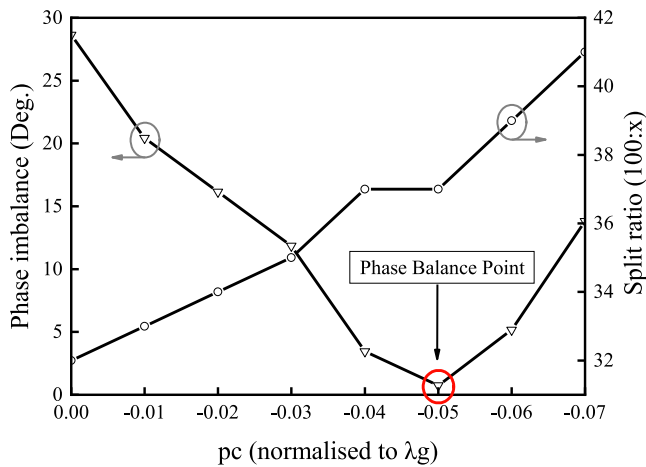


**FIGURE 4** Phase imbalance compensation by varying  $pc$  for 100:37 split ratio

step with the  $S$ -parameter responses presented in Figure 5(a) for the highest required split ratio of 100:37.

## 2.2 | Phase compensation

In order to compensate the phase imbalance of  $23^\circ$  from Step 1, the second step starts with a little larger split ratio of 100:32. Then this phase imbalance is compensated by slightly moving the inductive post and the input window as a batch (highlighted) by  $pc$  in the negative  $x$ -axis, while keeping the same relative distance as shown in Figure 2(c). As depicted in Figure 4, the phase balance point was found to be moving  $pc$  by only  $0.05 \times \lambda_g$  (guided wavelength) in the  $-x$ -direction; this will also lower the split ratio to the required 100:37. This process offers simple design solution and doesn't require any additional posts for phase balancing or additional step for port impedance matching, in comparison with [13]. The  $S$ -parameter responses after the phase balance were depicted in Figure 5(b). By using this proposed technique, the phase balance points

**TABLE 2** Design parameters

Parameters	Stage S1	Stage S2	Stage S3	Stage S4
Split ratio	100:100	37:100	41:100	78:100
$pd$ ( $\lambda_g$ )	0	0.153	0.137	0.038
$pc$ ( $\lambda_g$ )	0	-0.052	-0.044	-0.009

were optimised in simulations for all the required split ratios as shown in Table 2. It can be observed that with a lower split ratio, the required compensation distance  $pc$  will also be smaller.

## 2.3 | Eight-way unequal divider design

After analysing the individual Y- and T-dividers for the required split ratios, the obtained parameter values ( $pc$  and  $pd$ ) were implemented into the eight-way divider model in the following route. Due to the symmetry, the stage S1 division remained uniform. Thereupon, stage S2 was kept uniform strategically, and the  $pd$  and  $pc$  values from Table 2 were applied into the individual stages S3 and S4 as the third step. Fine tunings on  $pd$  and  $pc$  were then performed to achieve the targeted split ratios. Upon confirming the topmost power ratios, the splitting parameters were then inserted into stage S2, then being fine adjusted to match the port amplitude coefficients. This strategy will simplify the entire design process with less time-consuming optimisation. Therefore, this design process is suggested to begin with top splitters for optimisation rather than initiating from stage two (S2) as suggested in [12], the reason being the former procedure makes it easier to identify which splitter needs further tuning. The process could also begin chronologically from S1 to S4. However, locating the divider block which required tuning was quite difficult and it led to a time-consuming optimisation iteration. Additionally, each divider stage has its own influences on the complete divider network, which might reduce the overall bandwidth. The amplitude and phase responses of the finalised eight-way divider are depicted in Figure 5(c) for  $-35$  dB SLL. The CST simulation model is shown in Figure 6(a), where the end launched SubMiniature version A (SMA) connectors used are modelled according to the data sheet provided, so that the test jig can be designed precisely to ensure reliable measurement results.

## 3 | FABRICATION AND RESULTS

To verify the proposed method, the  $-35$  dB SIW eight-way power divider was fabricated as shown in Figure 6(b). The tapered transition between the SIW and microstrip line was used. The output ports were spaced by bending the legs outward from the adjacent ports for the SMA connections. A jig was 3D printed for the housing of the divider and fixed with the screw holes of plastic material for avoiding undesired influences. This is necessary as Taconic TLX-8 substrate is very soft and its RF transmission behaviour is sensitive to substrate bending. The divider responses were measured by an Agilent PNA E8361 A vector

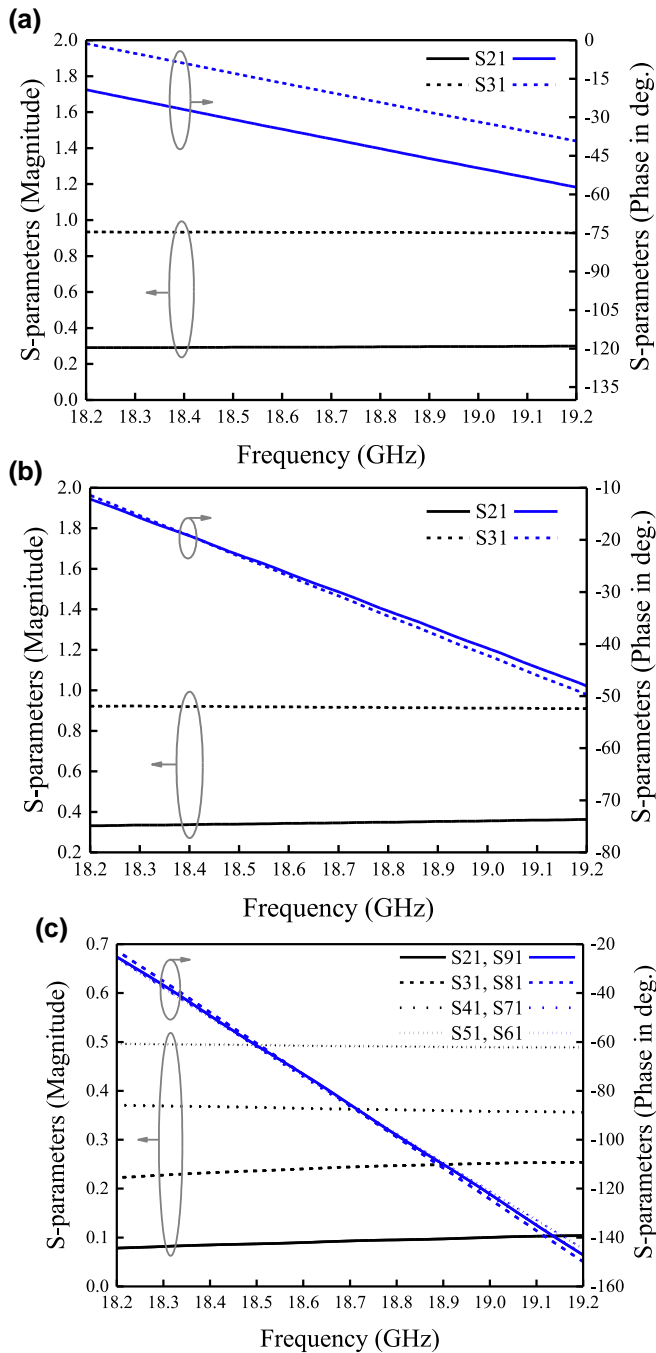


**FIGURE 5** Simulated  $S$ -parameter response of Y-divider: (a) after step 1 for unequal split; (b) step 2 for phase balancing and (c) balanced phase unequal split eight-way divider

network analyser. The individual port responses were measured by terminating the rest of the ports with  $50\ \Omega$  loads.

Figure 7 depicts the return loss performance of the power divider where the simulated and measured results were in good agreement. The measured return loss bandwidth ( $-15\ \text{dB}$ ) was from 15.5 to 22.5 GHz (36.8%); this is much improved as compared to 9% in [12]. It is worth noting that, for lower side-lobe resonant array antenna, the co-phase bandwidth is very important to maintain the lower side-lobe performance and resist the antenna array from the beam squint. Figure 8 shows

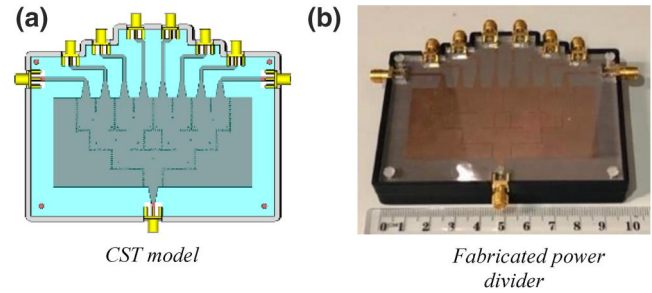


**FIGURE 6** The unequal ( $-35\ \text{dB}$ ) substrate integrated waveguide power divider

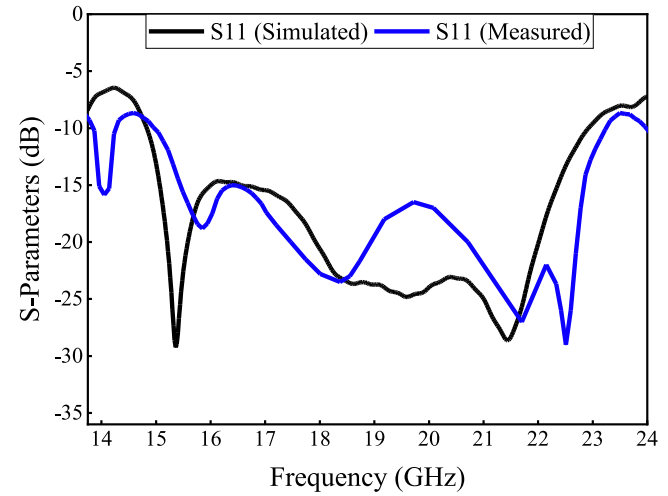


**FIGURE 7** Return loss response of the eight-way power divider

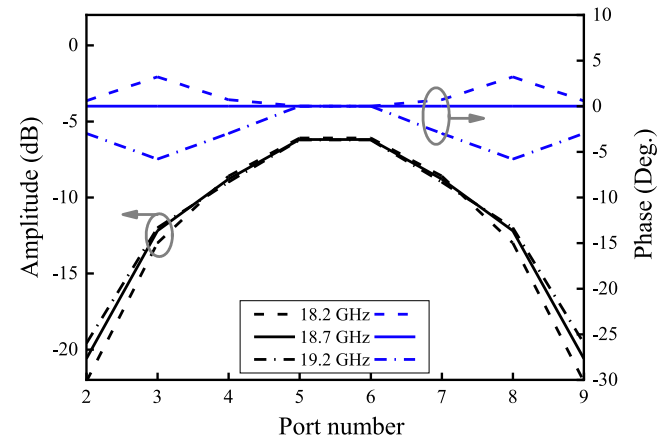


**FIGURE 8** Measured amplitude and phase responses of each ports

the amplitude and phase response of the individual divider ports. The maximum power difference was 14.4 dB ( $|\Delta\text{Out}| = |S_{51} - S_{21}|$ ) at 18.7 GHz and varied from 16 to 13.5 dB for 18.2 to 19.2 GHz. The phases were normalised with respect to the response of ports 5 and 6 for clarity.

The measured phase error between ports was less than  $5^\circ$  from 18.2 to 19.2 GHz and  $10^\circ$  from 17.7 to 19.6 GHz, exhibiting co-phase bandwidth of 6% and 10%, respectively. In

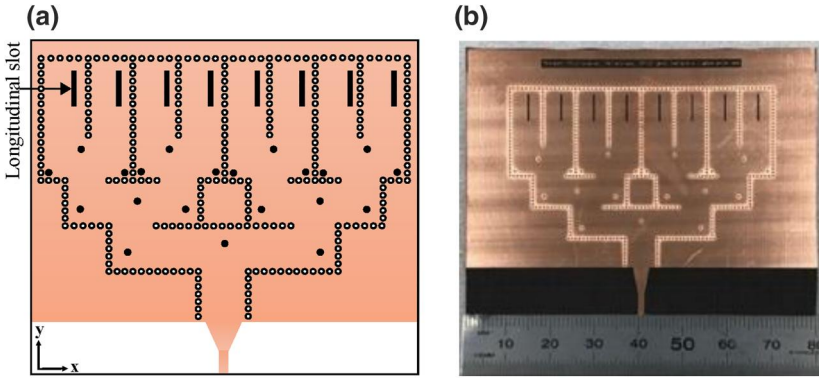


**FIGURE 9** The  $8 \times 1$  substrate integrated waveguide antenna array: (a) layout and (b) the fabricated antenna prototype

comparison, maximum of 4% co-phase bandwidth within  $13^\circ$  phase error was reported in [12]. Therefore, the enhanced co-phase bandwidth and wideband return loss response show significant improvement on the unequal power divider design; at the meantime, the proposed design method is more efficient than the conventional approach.

#### 4 | LINEAR ARRAY ANTENNA DESIGN AND RESULTS

The designed unequal power divider was integrated with the longitudinal radiating slots as a prototype to evaluate the performance of this power divider in terms of the antenna side-lobe reduction and main beam stability. The power divider ports were terminated with conductive via walls and the radiating elements were placed in  $\lambda_g/4$  distance from the shorted via walls. The resonant conductance of the end-fed slot was 1 and the resonant slot length (6.75 mm) was calculated using the equation from [22]. The slot width was designed to be 0.4 mm to meet the required bandwidth. Due to the surface current null at the centre of the SIW in every quarter-wave distance from the shorted wall, the slots were slightly displaced by following the guidelines provided in [23]. The eight-element linear array antenna was simulated and optimised using the commercial CST microwave studio suite and, later fabricated for practical verification. Figure 9 shows the layout and the fabricated prototype of the SIW linear array antenna.

Figure 10(a) compares the simulated and measured return loss response of the antenna array. The variation on slot widths affect the antenna bandwidth and the cross-polarisation level. The antenna model was fabricated with higher precision to ensure the slot widths are consistent to the simulated model. Both the simulated and measured return loss ( $-10$  dB) responses demonstrate good agreement with a bandwidth of 400 MHz, ranging from 18.5 to 18.9 GHz. For the application of radiometer, 18.6–18.8 GHz is the conventional bandwidth in Ku-band (being the secondary use for active radiation and hence less radio frequency interference) [24]. Additionally, the antenna exhibits better than  $-1.3$  dB (74%) radiation efficiency throughout the bandwidth. Therefore, this antenna design suits for the Ku-band radiometer system. The normalised simulated and measured

radiation patterns of the antenna array are shown in Figure 10(b, c), respectively.

Figure 10(b) compares the simulated radiation patterns of an SIW antenna with uniform and non-uniform (unequal) power distribution. It can be observed that the SLL was suppressed from  $-12$  to  $-27$  dB by using the unequal eight-way power divider from the previous section, which satisfies the design goal of  $-25$  dB SLL. The  $-3$  dB beam width was increased from  $13.5^\circ$  to  $18.1^\circ$ , while suppressing the SLL at the E-plane. The measured antenna radiation patterns are presented in Figure 10(c). The far-field radiation pattern was measured in a mm-wave anechoic chamber with a resolution of  $1^\circ$  rotation. The measured radiation pattern exhibits no beam squint from 18.6 to 18.8 GHz, which agrees with the simulated response. The measured peak gain of the antenna is about 13.45 dBi compared to the simulated gain of 14.2 dBi with a reduced SLL of  $-26.4$  dB. BE in Figure 10(b) stands for antenna beam efficiency that can be defined as [5]

$$BE(\theta_1) = \frac{\int_0^{2\pi} \int_0^{\theta_1} D(\theta, \phi) \sin\theta d\theta d\phi}{\int_{\phi=0}^{2\pi} \int_{\theta=0}^{\pi} D(\theta, \phi) \sin\theta d\theta d\phi} \sqrt{b^2 - 4ac} \quad (3)$$

where  $\theta_1$  is the angle of first minimum and  $D(\theta, \phi)$  is the directivity of the antenna in all directions. However, for the scope of demonstrating a tapered  $8 \times 1$  SIW antenna, the discussion of beam efficiency is confined to only the E-plane, which combines eight radiation patterns (in a row) to form a narrow beam, while only one radiating element (one column) can be seen in the H-plane with a wide beam pattern, and it is hence not discussed in this paper. By considering only the E-plane, as a result of SLL suppression, the beam efficiency was increased from 33% to 97%. This directly affects the antenna noise temperature ( $T_A$ ), which can be expressed as follows [25]:

$$T_A = T_B(\theta, \phi)BE_{\theta_1} + T_B(\theta, \phi)[1 - BE_{\theta_1}] \quad (4)$$

where  $T_B(\theta, \phi)$  is the thermal radiation equivalent (brightness) temperature from (objects) in all direction surrounding the antenna (but also confined to E-plane in this case). This improvement reflects that 97% of the antenna noise temperature is contributed by the antenna main lobe, while only 3% is from the side lobes and back lobes. In the application of radiometers, beam efficiency above 90% is usually required to

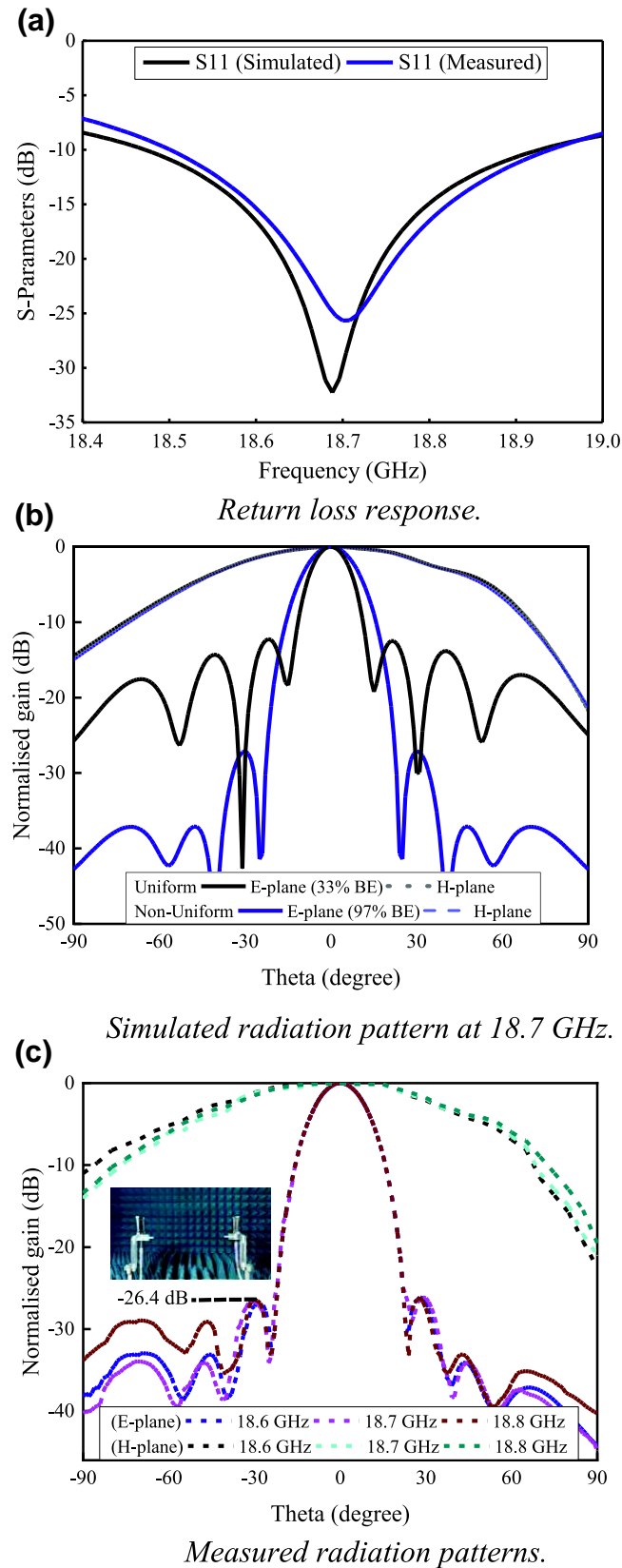


**FIGURE 10** The simulated and measured responses of the antenna array

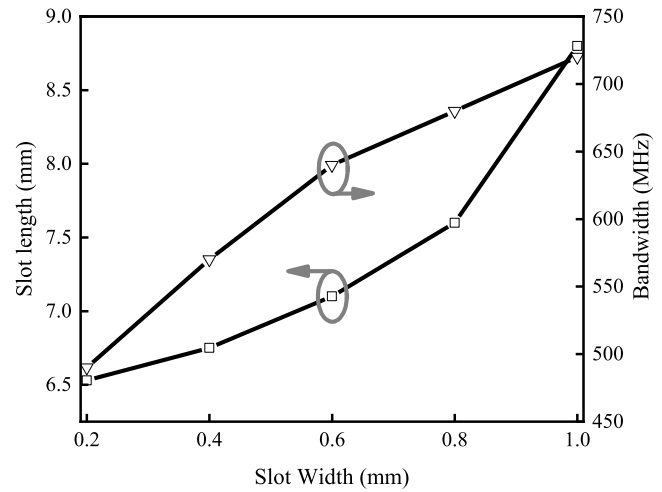


**FIGURE 11** Effects of the slot width on the slot length adjustment and bandwidth

ensure a reliable measurement of the pointing target (e.g., soil with  $T_B=200$  K), by minimising the effect of error from side and back lobes (e.g., typical sky with  $T_B=3$  K ; water with  $T_B=100$  K) [26]. Up to this stage, the deviation on the achieved SLL (as compared to the  $-35$  dB Chebyshev excitation) could possibly due to the higher order mutual coupling of the lower height waveguide, that is, SIW. This expected error can be minimised by following the Elliot's [27] and Jacob's [28] design methods, and it is possible to achieve better than  $-30$  dB of SLL value, and further improve the beam efficiency.

In addition, this proposed power divider has a large co-phased bandwidth (17.7–19.6 GHz) and return loss bandwidth (15.5–22.5 GHz). Its application can be extend to Ku-band radar [29] and satellite/wireless communications (with 17.8–19.7 GHz being the potential bandwidth for 5G network) [30,31], where highly directional and low SLL antennas are required. Further, the antenna bandwidth can be adjusted by tuning the antenna slot width as shown in Figure 11, and only for the context of radiometer that we utilised a narrow bandwidth.

## 5 | CONCLUSION

An improved co-phase bandwidth eight-way non-uniform substrate integrated power divider has been presented in this paper. An investigation on the unequal power division techniques was discussed for the high split ratios, on a basis of  $-35$  dB Chebyshev distribution algorithm. In comparison, the proposed design method exhibited lower phase imbalance and minimum variation on the ratio bandwidth, resulting lower optimisation complexity. The proposed eight-way unequal power divider has enhanced the co-phase bandwidth to 6% within  $5^\circ$  phase error and 10% within  $10^\circ$  phase error, and it has also demonstrated a wideband return loss response of 36.8%. Additionally, longitudinal slot radiators were initially

designed at 18.7 GHz and integrated with the designed divider network to demonstrate lower antenna side lobes. The SIW  $1 \times 8$  linear array antenna accomplished the goal of  $-25$  dB SLL at the E-plane, which improved the antenna beam efficiency from 33% to 97% with a gain of 13.45 dBi, and also, no beam squint is observed throughout the antenna operating bandwidth from 18.6 to 18.8 GHz. In addition, this antenna exhibits low simulated radiation loss of better than  $-1.3$  dB within the radiometer bandwidth. In conclusion, the proposed power divider demonstrated excellent credibility in improving antenna beam efficiency for the radiometer application. And also, it can be a potential candidate for Ku-band radar and satellite/wireless communications.

## ACKNOWLEDGEMENTS

This work has been supported by the Australian Research Council (ARC) under the Grant DP160104233. The authors would like to thank Dr. Mazyar Forouzandeh and Dr. Lilian Khaw for their technical support and helpful discussions. The authors would also like to thank all the reviewers for their comments and suggestions to improve this paper.

## ORCID

Shabriar Hasan Shehab  <https://orcid.org/0000-0001-9250-8335>

## REFERENCES

- Bayderkhani, R., Hassani, H. R.: Wideband and low sidelobe slot antenna fed by series-fed printed array. *IEEE Trans. Antenn. Propag.* 58(12), 3898–3904 (2010)
- Singh, A.: A low cost, low side lobe and high efficiency non-orthogonally coupled slotted waveguide array antenna for monopulse radar tracking. In: *IEEE Antennas and Propagation Society International Symposium*, vol. 3, pp. 732–735. IEEE (2005)
- Zetterstrom, O., et al.: Low-dispersive leaky-wave antennas for mmWave point-to-point high-throughput communications. *IEEE Trans. Antenn. Propag.* 68(3), 1322–1331 (2019)
- Hansen, R., Rudge, A.: Linear arrays. In: Rudge, A.W., Milne, K., Olver, A.D., Knight, P. (eds.) *The Handbook of Antenna Design*, Vol. 2, pp. 104–109. Peter Peregrinus Ltd., London (1983)
- Balanis, C.A.: *Antenna Theory: Analysis and Design*. John Wiley & Sons (2016)
- Pingree, P., et al.: Microwave radiometers from 0.6 to 22 GHz for Juno, a polar orbiter around Jupiter In: 2008 IEEE Aerospace Conference. IEEE (2008)
- Chamberlain, N., et al.: Juno microwave radiometer all-metal patch array antennas. In: *Antennas and Propagation Society International Symposium (APSURSI)*, pp. 1–4. IEEE (2010)
- Shigeki, F.: Waveguide line (in Japanese) Japan Patent 06-053, (1994)
- Uchimura, H., Takenoshita, T., Fujii, M.: Development of a laminated waveguide. *IEEE Trans. Microw. Theor. Tech.* 46(12), 2438–2443 (1998)
- Xu, J. F., et al.: Design and implementation of low sidelobe substrate integrated waveguide longitudinal slot array antennas. *IET Microw. Antennas. Propag.* 3(5), 790–797 (2009). <https://doi.org/10.1049/iet-map.2008.0157>
- Contreras, S., Peden, A.: Graphical design method for unequal power dividers based on phase-balanced SIW tee-junctions. *Int. J. Microw. Wirel. Technol.* 5(05), 603–610 (2013). <https://doi.org/10.1017/s1759078713000615>
- Yang, H., et al.: Improved design of low sidelobe substrate integrated waveguide longitudinal slot array. *IEEE Antenn. Wirel. Propag. Lett.* 14, 237–240 (2015). <https://doi.org/10.1109/lawp.2014.2360832>
- Park, S.J., Shin, D.H., Park, S.O.: Low side-lobe substrate-integrated-waveguide antenna array using broadband unequal feeding network for millimeter-wave handset device. *IEEE Trans. Antenn. Propag.* 64(3), 923–932 (2016). <https://doi.org/10.1109/TAP.2015.2513075>
- Yang, N., Caloz, C., Wu, K.: Substrate integrated waveguide power divider based on multimode interference imaging. In: *IEEE MTT-S International Microwave Symposium Digest*, pp. 883–886. IEEE (2008)
- Zou, X., Tong, C.M., Yu, D.W.: Y-junction power divider based on substrate integrated waveguide. *Electron. Lett.* 47(25), 1375–1376. (2011). <https://doi.org/10.1049/el.2011.2953>
- Zhu, F., et al.: Design and implementation of a broadband substrate integrated waveguide magic-T. *IEEE Microw. Wirel. Compon. Lett.* 22(12):630–632 (2012)
- Song, K., et al.: Wideband out-of-phase SIW power divider with enhanced stopband. In: *2013 IEEE International Wireless Symposium (IWS)*, 14–18 April 2013, pp. 1–3. IEEE (2013). <https://doi.org/10.1109/IWS.2013.6616702>
- Djerafi, T., et al.: Ring-shaped substrate integrated waveguide Wilkinson power dividers/combiners. *IEEE Trans. Compon. Packag. Manuf. Technol.* 4(9), 1461–1469 (2014)
- Chen, X., et al.: Development of compact HMSIW Gysel power dividers with microstrip isolation networks. *IEEE Access.* 6, 60429–60437 (2018). <https://doi.org/10.1109/ACCESS.2018.2875268>
- Xu, F., Wu, K.: Guided-wave and leakage characteristics of substrate integrated waveguide. *IEEE Trans. Microw. Theor. Tech.* 53(1), 66–73 (2005)
- El-Hajj, A., Kabalan, K.Y., Al-Husseini, M.: Generalized Chebyshev arrays. *Radio Sci.* 40(3), 1–8 (2005)
- Farrall, A., Young, P.R.: Integrated waveguide slot antennas. *Electron. Lett.* 40(16), 1 (2004)
- Stevenson, A.: Theory of slots in rectangular wave-guides. *J Appl. Phys.* 19(1), 24–38 (1948)
- Ulaby, F.T.: Microwave remote sensing active and passive. In: Ulaby, F.T., Moore, R.K., Fung, A.K. (eds.) *Radar Remote Sensing and Surface Scattering and Emission Theory*, pp. 848–902. Addison-Wesley Publishing Company, Advanced Book Program/World Science Division (1982)
- Volakis, J.L., Johnson, R.C., Jasik, H.: *Antenna Engineering Handbook*. McGraw-Hill Education (2007)
- Skou, N., Le Vine, D.: *Microwave Radiometer Systems, Design and Analysis*. Artech House (2006)
- Elliott, R.: An improved design procedure for small arrays of shunt slots. *IEEE Trans. Antenn. Propag.* 31(1), 48–53 (1983)
- Coetzee, J.C., Sheel, S.: Waveguide slot array design with compensation for higher order mode coupling between inclined coupling slots and neighboring radiating slots. *IEEE Trans. Antenn. Propag.* 67(1), 378–389 (2018) <https://mpd.southwestmicrowave.com/product-category/end-launch-connectors/>
- Zulkefley, N.R., et al.: Channel characterization for indoor environment at 17 GHz for 5G communications. In: *IEEE 12th Malaysia International Conference on Communications (MICC)* 241–245. IEEE (2015)
- Garcia-Marin, E., Masa-Campos, J.L., Sanchez-Olivares, P.: Planar array topologies for 5G communications in Ku band [wireless corner]. *IEEE Antenn. Propag. Mag.* 61(2), 112–133 (2019)

**How to cite this article:** Shehab SH, Feng J, Karmakar N, Amin EM, Walker J. Improved wideband phase balancing SIW unequal power divider design for the low side-lobe array antennas. *IET Microw. Antennas Propag.* 2021;15:115–122. <https://doi.org/10.1049/mia2.12027>